Influence of Microalloying and Heat Treatment on the Kinetics of Bainitic Reaction in Austempered Ductile Iron

B. Bosnjak, B. Radulovic, K. Pop-Tonev, and V. Asanovic

(Submitted 24 May 2000)

The effect of different contents of alloying additions and austenitizing temperature on the transformation kinetics of austenite in a ductile iron austempered at 300 and 400 °C has been investigated in the present study. X-ray diffraction, optical microscopy, and hardness measurements were used to determine the transformation kinetics of low Ni iron, low Mo iron and low Ni, Mo iron during austempering at 300 and 400 °C for 1 to 480 min after austenitizing at 850 and 930 °C for 120 min. Nickel and molybdenum in used contents are shown to delay the bainitic transformation without the undesirable features. Decreasing the autenitizing temperature is shown to increase the driving force for stage I of reaction but to have only a small effect on stage II kinetics. This shifts the position of the processing window to short periods of time and leads to opening of the processing window, which is closed for higher autenitizing temperatures. A more uniform austempered microstructure can be obtained with a decrease of autenitizing temperature. Decreasing the autenitizing temperature has the disadvantage of reducing the austemperability.

Keywords ADI microalloying, ductile iron

1. Introduction

Heat treating the ductile cast iron produces austempered ductile irons (ADI), which have outstanding mechanical properties that can be varied over a wide range by varying the heat treatment parameters. They show an excellent combination of strength, fracture toughness, and wear resistance for a wide variety of applications in automotive, rail, and heavy engineering industries.[1–5]

The processing of ADI may give rise to significant economic advantages in the production of manufactured components. Austempered ductile iron is used to replace case-hardened steel forging for the manufacture of rear axles and has been reported to produce a 50% energy saving; *i.e.*, more energy is required to produce a steel forging (even without heat treatment) than is required for the casting and austempering of a ductile iron component. Machining costs are also generally lower because of the unique microstructure due to less tool wear and increased machine shop capacity. Overall, a cost reduction of 30% is expected from the replacement of forged steel crankshafts by ADI.

With these economic advantages, it is not surprising that ADI is being used, worldwide, for an increasing range of high-performance applications.

At present, this relatively new material is only a small fraction of the ductile iron market but is expected to grow, as machining and heat-treatment facilities become available in more foundries.

B. Bosnjak, V. Asanovic, and **B. Radulovic,** University of Montenegro, Rektorat Cetinjski put bb 81 000 Podgorica, Yugoslavia; and **K. Pop-Tonev,** Department of Technology and Metallurgy, University "Rudjer Boskovic," 91 000 Skopje, Macedonia. Contact e-mail: bosnjakb@cg.ac.yu.

2. Reaction of Austempering

Heat treatment of austempering basically consists of autenitizing ductile iron in the temperature range 850 to 950 °C, quenching to the austempering temperature in the range 250 to 400 °C for a controlled time, and then cooling to room temperature (Fig. 1).

During autenitizing, the as-cast matrix structure transforms either into austenite or a mixture of proeutectoid ferrite and austenite. The autenitizing step in the treatment of ductile iron differs from that in a steel because the austenite carbon content in an iron (0.6 to 1.1%) depends on the iron composition and autenitizing temperature.

During the austempering process, ADI undergoes a two-stage transformation process.[4,5] In the first stage, the austenite (γ) decomposes into bainitic ferrite (α) and carbon-enriched austenite (γ_{hc}), a product known as ausferrite. This reaction can be expressed as

$$\gamma \rightarrow \alpha + \gamma_{hc} \qquad \text{(Eq 1)}$$

If the casting is held at the austempering temperature for too long, then the carbon enriched austenite (γ_{hc}) further decomposes into ferrite (α) and carbide.

$$\gamma_{hc} \rightarrow \alpha + \text{carbide} \qquad \text{(Eq 2)}$$

Transitional carbide such as ε-carbide often forms in the early stages followed by a noncoherent carbide such as Fe_3C.

The optimum mechanical properties can be achieved upon completion of the first reaction, but before the second reaction.

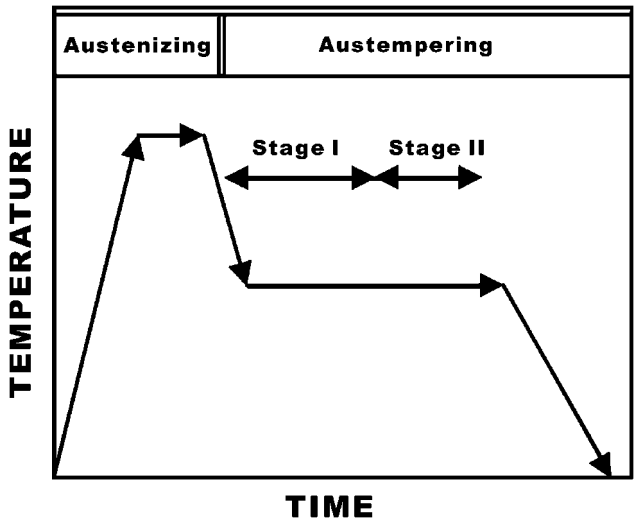

Fig. 1 Schematic diagram of the austempering process for cast iron

The second reaction produces carbides, which makes the material very brittle. This reaction is, therefore, undesirable and must be avoided. The time period between the end of stage I and the onset of stage II is called the processing window.

An important parameter in the austempering process is the chemical composition. The maximum section size that can be austempered without the formation of eutectoid and proeutectoid products depends primarily on the alloying additions.

Although sufficient alloying additions can be made to provide adequate austemperability, their presence can influence the austempering kinetics adversely, leading to reduction in mechanical properties. The main problem is associated with the strong segregation of alloying elements in the intercellular regions during solidification. These segregations are not removed during the period of autenitizing and produce heterogeneity of the structural matrix. Previous studies have shown that alloying elements postpone at the beginning of the stage I reaction.[4–6] This can lead to closure of the processing window and a reduction in mechanical properties. In practice, limiting the alloying additions has minimized the problem.

In ductile iron, tight control of the autenitizing temperature is imperative if consistent properties are to be maintained. The variations in autenitizing temperature shift the processing window over which optimum properties can be attained. In general, increasing the autenitizing temperature delays the austempering transformation and shrinks the size of the processing window.

The autenitizing temperature has a significant effect on the austemperability and transformation behavior at higher temperatures: the matrix carbon content increases and the austenite grain size is enlarged. This increase increases austemperability and reduces the rate of reaction, thus permitting larger castings to be treated or less efficient quenching baths to be used.[7]

The autenitizing temperature should be selected to ensure sufficient carbon transfer from the graphite nodules to the austenite matrix. The carbon solution process is both time and temperature dependent; thus, high autenitizing temperatures shorten the time necessary to attain a uniform carbon content in the matrix structure. However, scaling and casting distortion may result if autenitizing is carried out at higher temperatures.[8]

Lower austenitizing temperatures may be specified for castings which are to be machined after austempering. Lowering the autenitizing temperature lowers the volume of untransformed austenite. Under the higher pressures involved in machining, the untransformed austenite would transform to martensite, thus reducing machinability. On the other hand, a decrease in autenitizing temperature frequently results in incomplete austenitization and associated microstructural and low property problems.

The main objective of the present work is to study the effect of alloying additions (Ni and Mo) when they are added particularly or in combination and the effect of austempering parameters on austemperability, transformation kinetics, and the processing window.

3. Experimental

3.1 Casting Procedure

Three alloys of ductile iron used in the present work were produced in a medium frequency induction furnace of 100 kg capacity. The charge consisted of 50% pig iron ingot and 50% low manganese steel scrap. The melt was treated with 1.8% of magnesium ferrosilicon alloy using the sandwich technique. The melt was then inoculated with 0.67% foundry grade Fe-Si containing nominally 75% Si and cast at 1400 °C into a standard Y-block mold, which ensured a sound casting.

Image analysis techniques were used to measure the volume fraction of ferrite, pearlite, carbides, graphite, and the nodule count in the as-cast structures.

The segregation profiles for alloying elements (silicon, manganese, nickel, and molybdenum) between the intercellular region and the nodule, were measured, using scanning electron microscope (SEM) with energy dispersive x-ray spectroscopy (EDAX).

3.2 Austemperability

The effects of alloying additions and autenitizing temperatures on austemperability (critical bar diameter that can be austempered without pearlite formation) were investigated in a present work. Austemperability has been examined by Voight and Loper,[6] who suggest the following regression function for calculating the critical bar diameter:

$$\begin{aligned} D_c = {} & 124C_\gamma^\circ + 27(\%Si) + 22(\%Mn) + 16(\%Ni) \\ & + 25(\%Mo) + 1.68 \times 10^{-4}T_a^2 + 12(\%Cu)(\%Ni) \\ & + 62(\%Cu)(\%Mn) + 88(\%Ni)(\%Mo) \\ & + 11(\%Mn)(\%Cu) + 127(\%Mn)(\%Mo) \\ & - 20(\%Mn)(\%Ni) - 137 \end{aligned} \quad \text{(Eq 3)}$$

where C_γ° is the C content in the matrix austenite at the autenitizing temperature and T_a is the austempering temperature. The austenite C content depends on the autenitizing temperature T_γ and iron composition. This dependence is frequently described by the approximate expression

$$C_\gamma^\circ = T_\gamma/420 - 0.17(\%Si) - 0.95 \qquad \text{(Eq 4)}$$

3.3 Heat Treatment

Test specimens were initially austenitized for 2 h at 850 and 930 °C in a muffle furnace and then imminently austempered in a molten salt bath at 300 and 400 °C for, 1, 10, 30, 60, 120, 240, 360, and 480 min and finally air-cooled to room temperature.

Austempering using surface grinding removed any decarburized skin that may have formed during heat treatment. In order to avoid the transformation of any metastable austenite to martensite, the grinding speed was kept as low as practical.

3.4 Kinetic Study

Specimens for the kinetic study of the treated ductile irons were machined from the test section of the Y-block. The cutting operation was carried out slowly and under liberal cooling to minimize heating and machining stress. The specimens were ground to 1200 grade using water-lubricated silica carbide paper and etched in 90% hydrogen peroxide plus 10% concentrated sulfuric acid for 10 to 15 min. This technique removed the work-affected surface and at the same time minimized the occurrence of the textured structure.

In order to determine the volume fraction of retained austenite, x-ray diffraction analysis was carried out with Cu K_α radiation at 40 kV and 20 mA. The diffractometer was equipped with a strip chart recorder in the angular 2θ range of 20 to 120°. The profiles were computer analyzed to obtain the peak positions as well as the integrated intensities. The volume fraction of retained austenite X_γ was determined by the direct comparison method using integrated intensities of the (110) and (211) peaks of ferrite and the (111), (220), and (311) peaks of austenite. The carbon content of the austenite was determined using the relationship[9]

$$a_\gamma = 0.3548 + 0.0044\ C_\gamma \qquad \text{(Eq 5)}$$

where a_γ is the lattice parameter of austenite in nanometers and C_γ is its carbon content (wt.%). The (111), (220), and (311) peaks of austenite were used to estimate the lattice parameter.

For microstructural analysis, samples were taken from the impact test specimens at positions far from the fractured area. Specimens for light microscopy were prepared by the standard metallographic technique.

The heat tinting the prepared samples after light etching in 2% nital improved phase identification. Heat tinting was achieved by heating in an oven with no atmosphere protection at 260 °C for 5.5 h and cooling to room temperature. With this technique, the various phases appear in different vibrant colors. These colors are as follows: untransformed austenite, light blue; reacted high carbon austenite, light brown; ferrite, beige; eutectic carbide, white or cream; and martensite, dark blue.

During point counting, at last 2000 points were counted at magnification of 500 times. The number of counts was increased with the decreasing volume fraction of untransformed austenite to maintain a low standard deviation.

Hardness measurements were made using a standard Vickers pyramid hardness tester with a load of 10 kg. Each measurement represents the average of ten indentations.

Table 1 Chemical composition of treated ductile irons, wt.%

Alloy	%C	%Si	%Mn	%P	%S	%Cu	%Cr	%Ni	%Mo
I	3.19	2.59	0.07	0.023	0.002	0.02	0.13	0.80	0.01
II	3.21	2.59	0.08	0.023	0.003	0.02	0.13	0.07	0.25
III	3.20	2.67	0.07	0.022	0.003	0.02	0.12	0.80	0.25

Table 2 Microstructural characteristics of as-cast ductile irons

Alloy	Graphite (vol.%)	Pearlite (vol.%)	Ferrite (vol.%)	Carbide (vol.%)	Nodule count (mm^{-2})
I	13	38	48	0.01	130
II	14	33	52	0.1	140
III	12	37	50	0.08	128

4. Results and Discussion

4.1 Characteristics of As-Cast Irons

The chemical compositions and microstructural characteristics of the three irons are given in Tables 1 and 2, respectively. The as-cast structure was of the typical bull's-eye type with ferrite surrounding the graphite nodules in pearlitic matrix with some carbides in the intercellular boundaries. The results in Table 2 are the averages from various locations in the discs of different thickness.

The line scans were made to show the solute distribution between graphite nodules (Fig. 2). Line scans show that Si and Ni segregate negatively during solidification; that is, more Si and Ni are found in areas close to graphite nodules in the center of the eutectic cell. On the other hand, Mo and Mn segregate positively during the solidification and more Mn and Mo are found in the last areas to solidify, the intercellular boundary area.

The austemperability is presented in Fig. 3 as the critical bar diameter that can be austempered without pearlite formation.

Combined Ni and low Mo additions achieve a significant increase in austemperability. A 23 mm diameter bar Ni iron, 21 mm diameter Mo iron, and 51 diameter Ni-Mo iron can be austempered at 400 °C after autenitizing 930 °C, without pearlite formation. These diameters are increased to 35, 33, and 61 mm, respectively, on reducing the austempering temperature to 300 °C, resulting in a higher quenching rate. The autenitizing temperature can also be seen to have a strong effect on austemperability. This is related to the influence of the autenitizing temperature on the origin carbon content. Decreasing the autenitizing temperature reduces austemperability.

4.2 Austempering Kinetics

Both effects of autenitizing temperature, on the driving force of the stage I reaction and austemperability, must be taken into account when selecting the autenitizing temperature for alloyed irons.

The volume fraction of retained austenite X_γ, the average

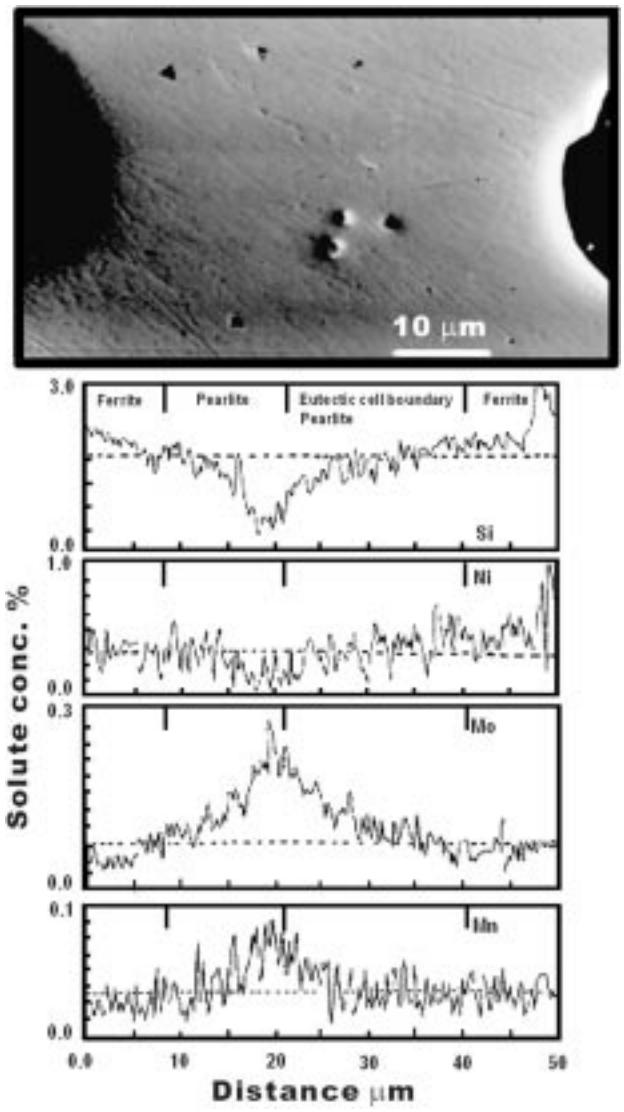

Fig. 2 As-cast microstructure Ni-Mo ductile iron and line scans between two graphite nodules

austenite carbon content C_γ, the volume fraction of untransformed austenite $X_{u\gamma}$, and the hardness were measured at 300 and 400 °C, after autenitizing at 850 and 930 °C for 120 min, and are shown in Fig. 4(a) to (h).

The change in measured parameters at short periods of austempering time (increase in X_γ and C_γ and decrease in $X_{u\gamma}$ and hardness) reflects the progress of the stage I reaction. The change at long periods of austempering time (slight increase in hardness and decrease in X_γ) are a consequence of the stage II reaction. As can be seen, little variation parameters at intermediate periods of austempering time in treated alloyed irons are evident. This has been attributed to solute segregation and its influence on kinetics of bainite transformation. The parameter changes at intermediate times reflect the completion of the stage I reaction in the eutectic cell, the beginning of the stage II reaction, and the reduction in blocky austenite areas, which form particularly at high autenitizing and high austempering temperatures.

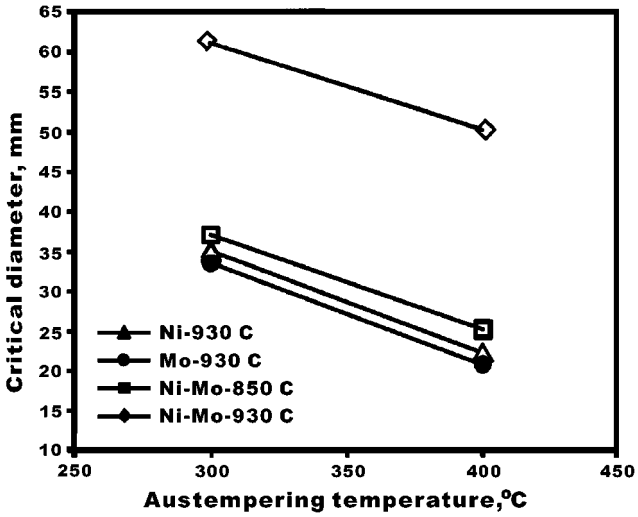

Fig. 3 Critical bar diameter above which pearlite forms during cooling from an autenitizing temperature of 850 and 930 °C for Ni, Mo, and Ni-Mo ductile irons

One of the most complex but most important aspects of austempering is the role of individual alloying elements and their interactive effects.[10]

4.3 Austempering Kinetics at 400 °C

Hardness measurements are used to determine the average stage I kinetics. We measured the time needed for the hardness to fall to 100 units above the minimum plateau level. The obtained value represented the time necessary for 60–80% of stage 1 reaction. These times are shown in Fig. 5 as a function of austempering temperature. Figure 5 shows that Ni and Mo delay the stage I reaction, which agrees with previous works.[11]

The effect of changing the autenitizing temperature from 850 and 930 °C can be measured in terms of the change in austenite carbon content. This autenitizing temperature change in the present irons increases the carbon content. These changes increase the time for completion of 60 to 80% of stage I reaction. The austenite carbon content can be controlled by the correct selection of the autenitizing temperature. Figure 5 shows that increasing the level of alloying elements increases the time for completion of 60 to 80% of stage I reaction. Previous studies[11] show that the early stages of the bainite transformations proceed in a manner that does not depend on the alloying elements present.

The completion of the stage I reaction is very important because it defines the beginning of the processing window. It can be followed by the fall in the untransformed austenite content. Figure 4(e) to (f) show that untransformed austenite content decreases sharply initially to a plateau or residual value before finally falling to a low level. It has been shown that the residual level is caused by the delay of the stage I reaction in the intercellular area and associated with the presence of Mo. The presence of untransformed austenite in the intercellular area can be seen in Fig. 6(a). Thus, austenite can be transformed to martensite during cooling to room temperature (Fig. 6b). This may be a primary reason for the difficulties in obtaining

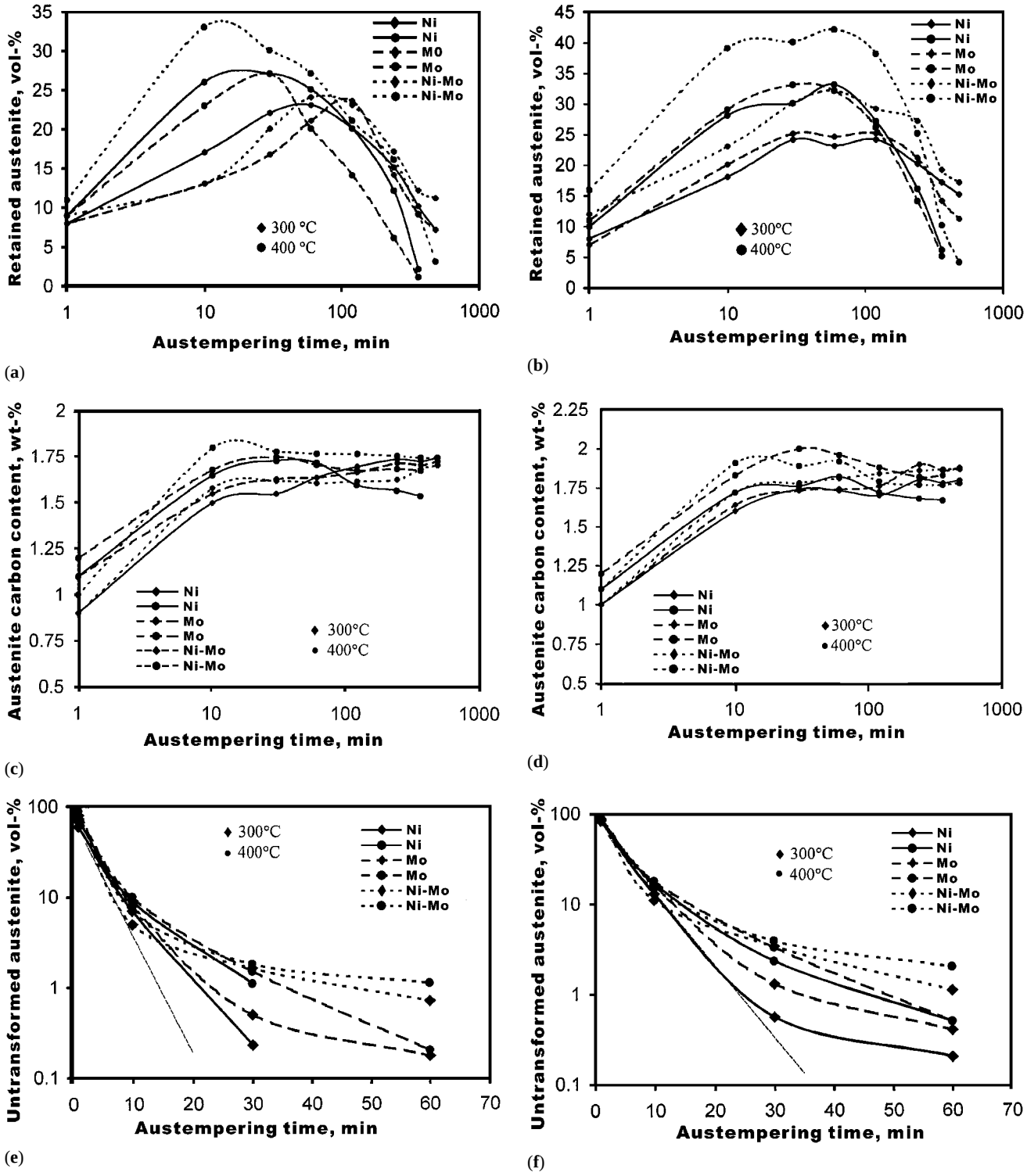

Fig. 4 Austempering kinetic measurements at 300 and 400 °C for Ni, Mo, and Ni-Mo irons austenitized (**a**), (**c**), (**e**), and (**g**) at 850 °C and (**b**), (**d**), (**f**), and (**h**) at 930 °C for 120 min. Variation with austempering time of (**a**) and (**b**) volume fraction of retained austenite, (**c**) and (**d**) carbon content of austenite, (**e**) and (**f**) volume fraction of untransformed austenite, and (**g**) and (**h**) hardness (continued on next page)

high ductility in Mo-alloyed irons austempered at high austempering temperatures (upper bainite range).[11,12] It is not the case with the used irons, because they contain small quantities of Mo 0.25%.

The curves that show untransformed, austenite content as a function of austempering time for the present irons can be divided into two separate groups of curves, one describing the stage I reaction in the eutectic cell and the second the stage I

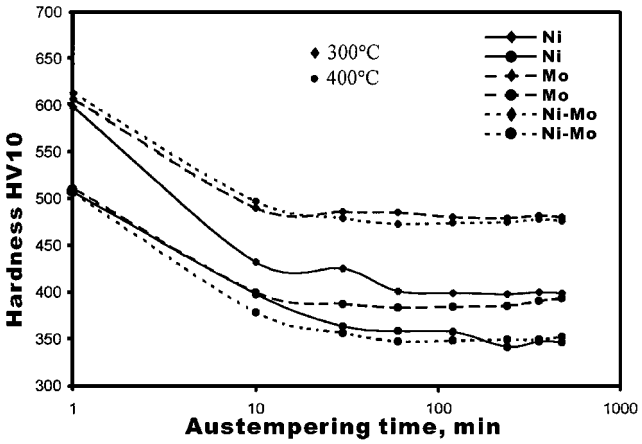

(**g**)

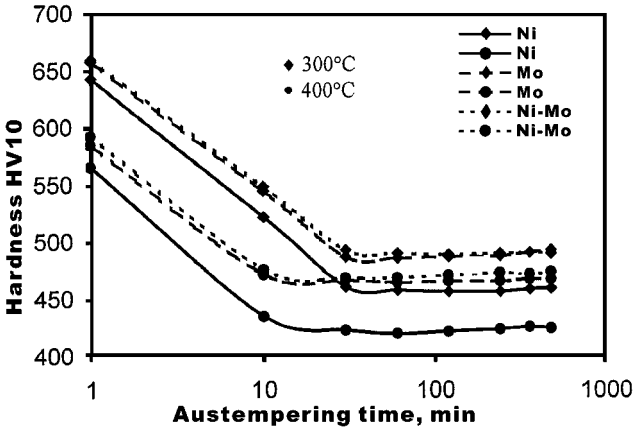

(**h**)

Fig. 4 Continued. Austempering kinetic measurements at 300 and 400 °C for Ni, Mo, and Ni-Mo irons austenitized (**a**), (**c**), (**e**), and (**g**) at 850 °C and (**b**), (**d**), (**f**), and (**h**) at 930 °C for 120 min. Variation with austempering time of (**a**) and (**b**) volume fraction of retained austenite, (**c**) and (**d**) carbon content of austenite, (**e**) and (**f**) volume fraction of untransformed austenite, and (**g**) and (**h**) hardness

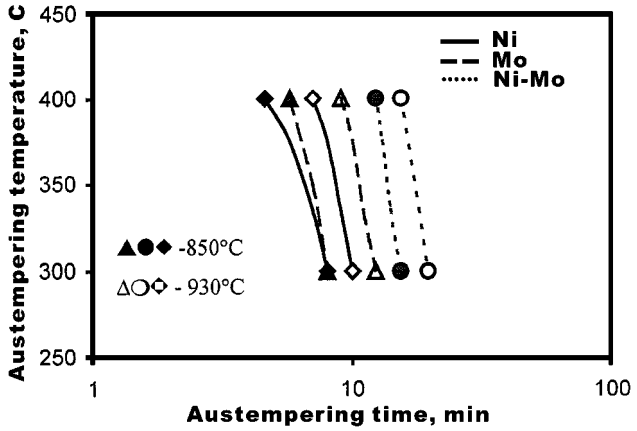

Fig. 5 Austempering time to fall to hardness of 100 units above the plateau value as a function of austempering temperature

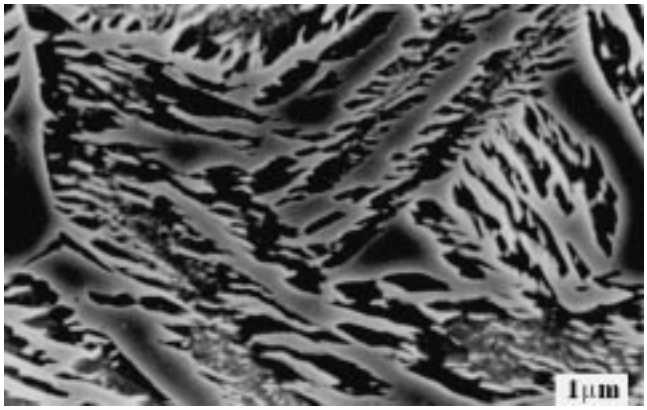

(**a**)

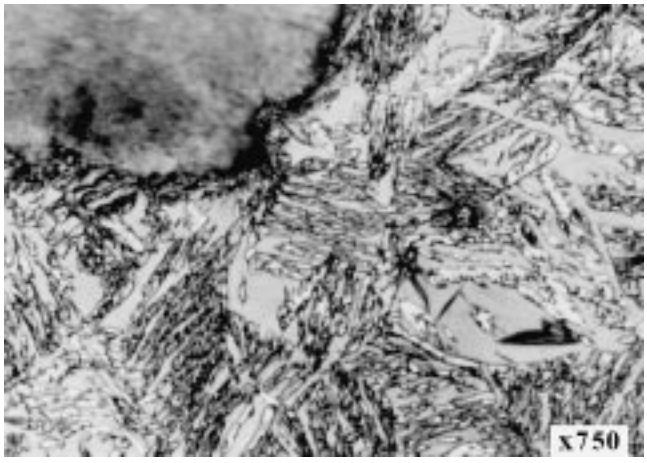

(**b**)

Fig. 6 Microstructure after austempering with (**a**) blocky retained austenite and (**b**) martensite within of blocky austenite

reaction in the intercellular area at longer periods of austempering time. The completion of stage I reaction in the eutectic cell can be estimated by extrapolating curves. The extrapolation shows that stage I reaction in the eutectic cell is completed (volume of untransformed austenite is 1%) after 17 to 55 mm. The figure also shows that reducing the autenitizing temperature to 850 °C reduces the time for the completion of the stage I reaction in the eutectic cell.

The decrease in untransformed austenite content at longer periods of austempering time for the same autenitizing and austempering conditions is shown in Fig. 4(e) and (f). The time for the completion of the stage I reaction in the intercellular region shows a strong dependence of autenitizing temperature. Decreasing the autenitizing temperature at the different austempering temperatures also reduces the level of untransformed austenite content in the intercellular region before completion of the stage I reaction.

Although Mo segregates to intercellular areas, it exerts very little influence on the driving force for stage I of bainitic transformation in quantities present in this study. Nickel does not segregate to intercellular regions and consequently all the curves in this figure (Fig. 4e and f) show a continuous decrease in

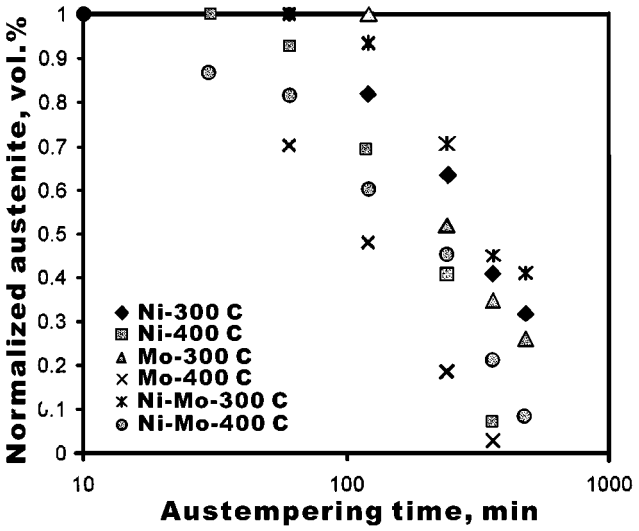

(**a**)

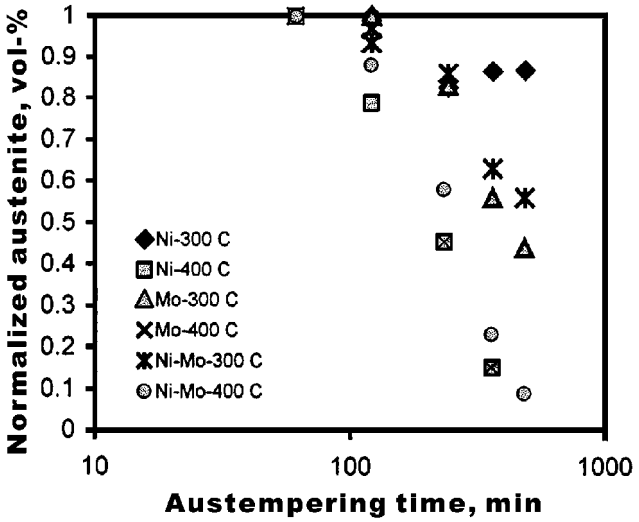

(**b**)

Fig. 7 Variation of volume fraction of normalized austenite X_γ/X_{max} with austempering time for given austempering temperatures: austenitized at (**a**) 850 °C and (**b**) 930 °C for Ni, Mo and Ni-Mo ductile irons

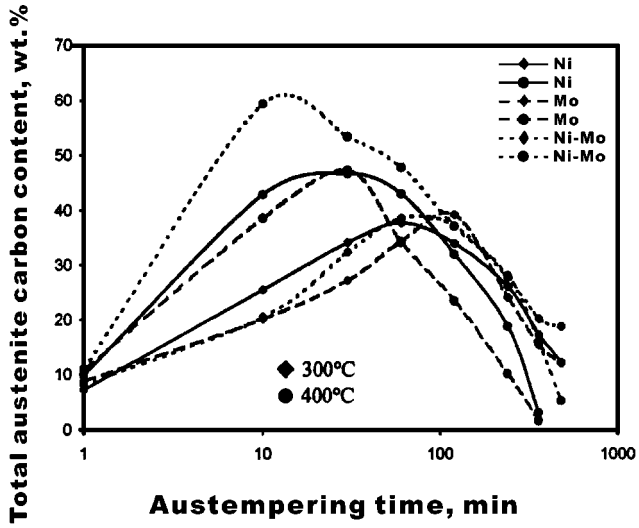

(**a**)

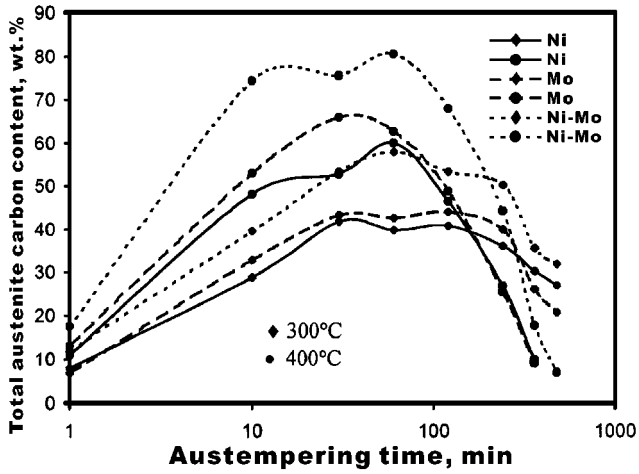

(**b**)

Fig. 8 Variation of total austenite content with austempering time at 300 and 400 °C austempering temperature, after autenitizing (**a**) 850 °C and (**b**) 930 °C for 120 min, for Ni, Mo, and Ni-Mo ductile irons

untransformed austenite content, indicating that alloying with Ni does not delay the completion of the stage I reaction. However, the figure does not show that, for three irons, as the austempering temperature increases, the rate of reduction of untransformed austenite content in the later stages of stage I decreases. This is associated with the formation of the blocky austenite. However, the decrease in untransformed austenite content is continuous, indicating that longer periods of austempering time, which promote carbon diffusion, will reduce untransformed austenite content and eliminate the martensite from the austempered structure.

The stage II reaction can be followed using the decrease in volume fraction of retained austenite in Fig. 4(a) and (b). The stage II reaction is a very sensitive function of the alloy content. It can be seen in Fig. 7, which shows a normalized austenite volume fraction (ratio volume fraction of retained austenite/maximum values of volume fraction of retained austenite) as a function of austempering time for given austempering conditions. It can be seen that the austempering temperature increases the rate of the stage II reaction, which contributes significantly to the closure of the processing window at higher austempering temperatures.

4.4 Austempering Kinetics at 300 °C

The measurements presented in Fig. 5 suggest that the stage I reaction in the eutectic cell is delayed at 300 °C compared with higher austempering temperatures. The maximum $C_\gamma X_\gamma$ values at 300 °C are much less than those at 400 °C, confirming the loss of carbon into carbides as the stage I reaction proceeds (Fig. 8). This figure also shows that the rate of change of $C_\gamma X_\gamma$ in the early part of the stage I reaction is slower at 300 than 400 °C. It is not possible to determine the initial rate of stage 1 reaction by conducting an analysis similar to that used for

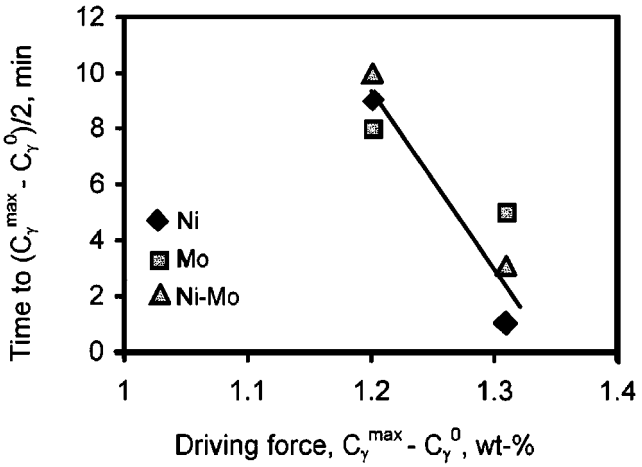

Fig. 9 Time to achieve austenite carbon content of $(C_\gamma^{max} + C_\gamma^\circ)/2$ as a function of driving force $C_\gamma^{max} - C_\gamma^\circ$ at austempering temperature 300 °C (irons austenitized at 850 and 930 °C)

400 °C, because the carbide formation invalidates the C mass balance calculation. This can be overcome by using the carbon content of austenite at the midpoint between C_γ° and C_γ^{max} to measure the initial rate of transformation in the stage I reaction, determined from Fig. 9.

The strong dependence on the driving force in the lower bainite range is evident. The initial rate of transformation in the stage I process is determined primarily by the driving force and is relatively independent of the alloying additions. Figure 5(c) and (d) show that the residual untransformed austenite content at 300 °C is less than that at 400 °C for the same autenitizing conditions. This is a consequence of higher driving force at the lower austempering temperature. Decreasing the autenitizing temperature at a constant austempering temperature shows the same effect.

It was found that at each autenitizing temperature the stage I reaction at 300 °C was delayed in the early stages of the reaction but occurred more quickly as it proceeded. The stage I reaction in the eutectic cell was found to take longer, particularly for the 930 °C autenitizing temperature. Decreasing the autenitizing temperature lowers the austempering time at which the 1% level of untransformed austenite content is achieved in the intercellular region. This level is achieved at 300 °C before it is at 400 °C at all autenitizing temperatures.

The stage II reaction shows a significant dependence of alloying additions. It can be seen in Fig. 4(a) and (b), which show that the decrease in retained austenite content is slower in Ni-Mo iron than in Ni iron and Mo iron. The stage II reaction at 300 °C occurs at a slower rate than at 400 °C. As with the stage II reaction at 400 °C, there is no clear dependence on autenitizing temperature.

4.5 Processing Window

The concept of the processing window was introduced originally by Rundman[13] to define the austempering time at which optimum mechanical properties, particularly ductility, were obtained. The beginning and end of the processing window are defined in terms of the amount of untransformed austenite in

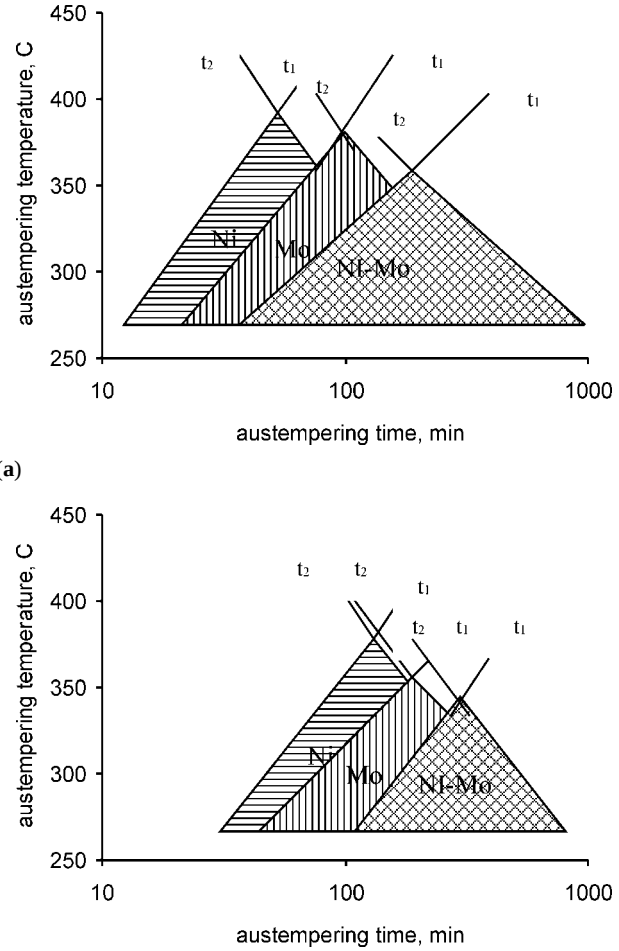

Fig. 10 Variation of processing window times t_1 and t_2 with austempering temperature for irons austenitized at (**a**) 850 °C and (**b**) 930 °C

the stage I reaction and the amount of bainitic carbide in the stage II reaction.

The criterion used to define the beginning of the window (t_1) is an untransformed austenite volume of 3%, which is determined from the relationship between untransformed austenite volume and austempering time measured using quantitative metallography. The criterion used to define the end of the processing window (t_2) is 90% of the maximum volume of retained austenite, measured using x-ray diffraction.[14] The horizontal line is constructed at a value of 10% below the level, which shows the largest values of retained austenite, intersecting the curve at times t_{min} and t_{max}. The value of t_2 is then defined by

$$\ln t_2 = (\ln t_{min} + \ln t_{max})/2 \qquad \text{(Eq 6)}$$

Figure 10(a) and (b) show the variation of t_1 and t_2 calculated using the above procedure for treated irons as a function of austempering temperature for different autenitizing temperatures.

Processing windows are relatively wide at 300 °C. They narrow and eventually close at 400 °C. Closure occurs at a 300 °C austempering temperature in complex (Ni-Mo) alloyed iron.

Lowering the autenitizing temperature increases the driving force for the stage I reaction, moving the processing window to earlier austempering times, especially for the 400 °C austempering temperature.

5. Conclusions

Irons containing 0.8% Ni, 0.25% Mo, or 0.8% Ni and 0.25% Mo are shown to have austemperabilities such that a 35, 33, and 61 mm diameter bar, respectively, can be austempered at 300 °C after autenitizing at 930 °C without pearlite formation.

Decrease in the austenitizing temperature reduces the austenite carbon content and the iron's austemperability. However, it increases the possibility of ferrite and pearlite formation during austempering heat treatment.

The rate of bainite transformation is controlled by the driving force $C_\gamma^{max} - C_\gamma^\circ$, where C_γ^{max} is the maximum carbon content of the austenite and C_γ° is the carbon content of the matrix austenite. The present measurement shows that the effect of Ni and Mo alloying elements on stage I kinetics is through their influence on the local carbon content of the austenite. Alloying elements, Ni and Mo, show a strong influence on the stage II reaction through their effect on the nucleation and grow of the ferrite and carbide phases from the high carbon austenite.

Decreasing the autenitizing temperature increases the driving force for the stage I reaction but does not have a clear effect on the stage II reaction.

The kinetics measurements are used to define the processing window according to the microstructural criterion. The austempering time corresponding to the beginning of the processing window t_1 is defined by measurements of volume fraction of untransformed austenite and that corresponding to closing of the window is defined based on carbide formation.

Nickel and molybdenum as alloying elements delay the appearance of the processing window.

Decreasing the autenitizing temperature moves the processing window to an earlier austempering time, which can open a processing window that is closed at the higher autenitizing temperature.

References

1. R.B. Gundlach and J.F. Janowak: *Met. Progr.*, 1985, vol. 12, pp. 231-36.
2. R.A. Harding: *Foundry Trade J.*, 1993, vol. 4, pp. 192-94.
3. J. Race and L. Stott: *Heat Treatment Met.*, 1991, vol. 18 (4), pp. 105-09.
4. B.V. Kovacs: *Trans. AFS*, 1994, vol. 102, pp. 417-20.
5. J.F. Janowak and R.B. Gundlach: *Trans. AFS*, 1983, vol. 86, pp. 377-88.
6. R.C. Voight and C.R. Loper: *Proc. 1st Int. Conf. on Austempered Ductile Iron*, ASM, Metals Park, OH, 1984, pp. 83-103.
7. J.F. Jonovak and P.A. Morton: *AFS Trans.*, 1985, vol. 88, pp. 123-35.
8. U. Draughlates and H.G. Boase: *2nd Int. Conf. on ADI*, Ann Arbor, Michigan, Mar. 1986.
9. B.D. Cullity: *Elements of X-Ray Diffraction*, Addison-Wesley, Reading, MA, 1978, pp. 350-68.
10. T.N. Rouns and K.B. Rundman: *Proc. Conf. "Transactions of the American Foundrymen's Society,"* American Foundrymen's Society, Des Plaines, IL, 1987, vol. 95, pp. 851-74.
11. N. Darwish and R. Elliott: *Mater. Sci. Technol.*, 1993, vol. 9, pp. 572-85.
12. A.S. Hamid and R. Elliot: *Mater. Sci. Technol.*, 1996, vol. 12, pp. 780-87.
13. D.J. Moore, T.N. Rouns, and K.B. Rundman: *AFS Trans.*, 1986, vol. 94, pp. 255-64.
14. Chan Tung Chen and Tien Shou Lei: *Mater. Trans., JIM*, 1999, vol. 40 (1), pp. 82-85.